

A dynamic nondestructive damage detection methodology for orthotropic plate structures

Amir Hossein Gandomi^{1a}, Mohammad G. Sahab^{*1} and Alireza Rahai^{2b}

¹Department of Civil Engineering, Tafresh University, Tafresh, Iran

²Department of Civil and Environmental Engineering, Amirkabir University of Technology, Tehran, Iran

(Received September 28, 2009, Accepted April 6, 2011)

Abstract. This paper presents a methodology to detect and locate damages and faults in orthotropic plate structures. A specific damage index based on dynamic mode shapes of the damaged and undamaged structures has been introduced. The governing differential equation on transverse deformation, the transverse shear force equations and the invariant expression for the sum of transverse loading of an orthotropic plate are employed to obtain the aforementioned damage indices. The validity of the proposed methodology for isotropic and orthotropic damage states is demonstrated using a numerical example. It is shown that the algorithm is able to detect damages for both isotropic and orthotropic damage states acceptably.

Keywords: damage detection; orthotropic plates; modal parameters; damage indices

1. Introduction

Preventing deterioration while, maintaining the serviceability of a structure and its health monitoring have appeared as an important issue in structural engineering. During the past few decades, serious research attempts have been conducted in the field of nondestructive damage detection (NDD) to impede malfunction or even abrupt failure of structures (Doebling *et al.* 1996). Most of NDD methods are comprised of visual inspection or localized experimental methods such as acoustic or ultrasonic methods, magnetic field methods, radiography, dye penetrant, eddy current methods or thermal field methods (Doherty 1987, Askeland 1994). When the approximate location of a damage is known, the accurate position and detailed information of the damage can be obtained, using these methods. In addition most local non-destructive testing (NDT) methods can only detect potential damage on or near the surface of the structures (Doebling *et al.* 1996, Choi *et al.* 2006).

Global damage detection methods are different techniques for structural damage identification (Gandomi *et al.* 2008). In these methods the general behavior of a structure is investigated to find out the existence, location and intensity of the damage. Generally, existing global damage detection methods can be classified in two major categories which are the dynamic and static damage

*Corresponding author, Assistant Professor, E-mail: sahab@aut.ac.ir

^aResearch Assistant, E-mail: a.h.gandomi@gmail.com

^bProfessor, E-mail: rahai@aut.ac.ir

identification methods. In the dynamic damage detection methods, changes in dynamic properties of the damaged structures are evaluated to detect the location and severity of the damages (Yan *et al.* 2007). In contrast the static damage detection techniques assess the changes of the static properties of the damaged structures to identify the location on severity of the damages (Sohn *et al.* 2003).

Vibration-based damage detection methods has evolved over the last three decades. These methods rely on the use of the natural frequencies and/or the mode shapes of the structures to identify damages (Cawley and Adames 1979, Stubbs 1985, Kim and Stubbs 1995b, Pandey *et al.* 1999, Kim *et al.* 2006, Zhao and Dewolf 2007).

Even though, to date, numerous NDD methods have been developed (Zou *et al.* 2000) but a few of them is devoted to plate-type structures. The first effort in this field was made by Cawley and Adams (1979). They introduced a method to locate the damages in a plate structure using frequency information. Chen and Swamidass (1994) used strain mode shapes to detect a crack in a cantilever plate. Choi and Stubbs (1997) presented two NDD methods for plate structures. One of these methods based on the differential equation of vibration of the plates and the other one uses the expression of elastic strain energy of a plate to detect damages. In addition to these theoretical research efforts, Cornwell *et al.* (1999) prepared some experimental research to verify the application of the damage index method to a plate structure. Two of the recent studies on damage detection in plate structures which have been attracted much attention have been conducted by Choi *et al.* (2005, 2006).

Many damage detection methods, represented in the literature for plate structures, are restricted to identify damages in isotropic plates. Araujo dos Santos *et al.* (2000) used both natural frequencies and vibration modes to detect the damages within a laminated rectangular plate. Lee *et al.* (2003) derived the equation of motion for the thin uniform rectangular plate with line crack-like damages with isotropic intact material. They represent, a local damage in terms of the effective orthotropic elastic stiffnesses. Yan *et al.* (2004) employed natural frequencies and dynamic responses for detecting small crack damages in a honeycomb sandwich plate. Yan *et al.* (2006) presented an improved method for establishing dynamic model of a structure with small damages. The proposed method has been implemented to identify damages in a laminated composite vessel.

The damage index method proposed by Stubbs *et al.* (1995) can be considered as an initiation for different group of damage detection techniques. This method is based on this fact that the fractional modal strain energy of a potential damaged element is invariant before and after a small damage event. This study introduces a damage index method applicable for isotropic and orthotropic plate like structures. A few specific damage indices based on dynamic mode shapes of the damaged and undamaged structures has been introduced. The governing differential equation on transverse deformation, the transverse shear force equations and the invariant expression for the sum of transverse loading of an orthotropic plate are employed to obtain the aforementioned damage indices. The validity of the proposed method for isotropic and orthotropic damages is demonstrated using numerical data.

2. Theory

2.1 The damage index method

The damage index method developed by Stubbs *et al.* (1992) utilizes the change in the modal

strain energy distribution due to damage. This method has been certified using numerically simulated data (Kim and Stubbs 1995a), experimental modal data generated in a laboratory environment (Kim and Stubbs 1995b), and field data measured on bridge structures (Choi *et al.* 2004). The extension of the damage index method for a plate structure was proposed by Choi and Stubbs (1997). They presented a strain-energy-based damage index. After that Choi *et al.* (2005, 2006) improved the damage index method by using compliance index and they introduce a new damage index. In the compliance index method, they utilized the relationship between the bending moments and the curvatures in a plate structure while in the new damage index method they used the relationship between the stiffness loss and the fractional changes of the modal parameters due to damage.

The above mentioned damage index methods are limited to isotropic plate structures, while this study presents a dynamic damage detection method for isotropic and orthotropic plate structures. Three new damage dynamic indices have been presented and used to locate damages in an orthotropic plate structure; however these indices can be simply used for isotropic plate structures as well.

2.2 Method of identification

Basically an orthotropic plate has different stiffness in two orthogonal directions. In practice a steel plate may be stiffened in one direction using some ribs to make an orthotropic plate as shown in Fig. 1. For an orthotropic plate structure, the governing differential equation of deflection is expressed in the form of (Ugural 1999)

$$D_x \frac{\partial^4 w}{\partial x^4} + 2H \frac{\partial^4 w}{\partial y^2 \partial x^2} + D_y \frac{\partial^4 w}{\partial y^4} = P \tag{1}$$

where

$$H = D_{xy} + 2G_{xy} \tag{2}$$

here w is the modal displacement in the transverse direction; D_x is the flexural rigidity in x direction; D_y is the flexural rigidity in y direction; D_{xy} is the twisting stiffness; G_{xy} is the torsional rigidity. Although Eq. (1) states a condition for static equilibrium of a plate, but also it can be

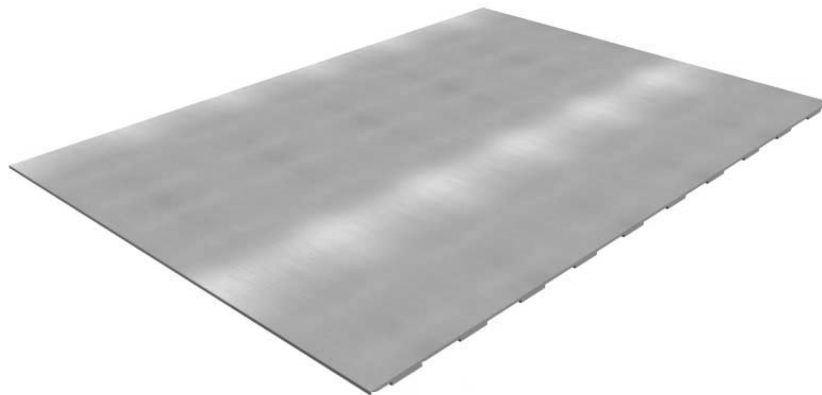


Fig. 1 Damage detection model of the example orthotropic plate structure

applied for its lateral vibration, considering d'Alembert's principle (Clough and Penzien 1995). According to this principle an accelerating rigid body can transform into an equivalent static system by adding the so-called inertial force and inertial torque or moment (Timoshenko and Woinowsky-Krieger 1959). In this case, P in Eq. (1) includes the external and inertial forces and w would be a function of the coordinates x and y and the variable of time, t . If Eq. (1) is applied to the equivalent static system at any specific time during vibration the variable of time is removed. In addition for the plate, the transverse shear forces can be stated as follows (Ugural 1999)

$$Q_x = -\frac{\partial}{\partial x} \left(D_x \frac{\partial^2 w}{\partial x^2} + H \frac{\partial^2 w}{\partial y^2} \right) \quad (3)$$

$$Q_y = -\frac{\partial}{\partial y} \left(D_y \frac{\partial^2 w}{\partial y^2} + H \frac{\partial^2 w}{\partial x^2} \right) \quad (4)$$

As explained already, according to d'Alembert's principle Eqs. (3) and (4) can be applied for vibration of plates, considering an equivalent static system. For an arbitrary element j in the 2D space the mean of a function sum associated with the element j can be written using the mean value theorem for integrals (Kaplan 1991)

$$\bar{F}_j = \frac{1}{\Delta A_j} \iint F dx dy = F_j(\hat{x}, \hat{y}) \quad (5)$$

By using the mean value theorem for integrals, for a 2D element in the plate subjected to load $P(x, y)$, the mean of the transverse load sum associated with the j^{th} element can be rewritten as follow

$$\bar{P}_j = \frac{1}{\Delta A_j} \iint P dx dy = P_j(\hat{x}, \hat{y}) \quad (6)$$

Evaluating Eq. (6) at the middle of elements with the coordinates $x = \hat{x}$ and $y = \hat{y}$ and substituting for $P(x, y)$ using Eq. (1) yields

$$P_j(\hat{x}, \hat{y}) = \frac{1}{\Delta A_j} \iint \left(D_x \frac{\partial^4 w}{\partial x^4} + 2H \frac{\partial^4 w}{\partial y^2 \partial x^2} + D_y \frac{\partial^4 w}{\partial y^4} \right) dx dy \quad (7)$$

Similarly, for the damaged structure

$$P_j(\hat{x}, \hat{y}) = \frac{1}{\Delta A_j} \iint \left(D_x^d \frac{\partial^4 w}{\partial x^4} + 2H^d \frac{\partial^4 w}{\partial y^2 \partial x^2} + D_y^d \frac{\partial^4 w}{\partial y^4} \right) dx dy \quad (8)$$

here d is the superscript for parameters of the damaged structure; Since the total load for the undamaged and damaged structures are equal, then it can be written as

$$1 = \frac{\iint_{\Delta A_j} \left(D_x^d \frac{\partial^4 w^d}{\partial x^4} + 2H^d \frac{\partial^4 w^d}{\partial y^2 \partial x^2} + D_y^d \frac{\partial^4 w^d}{\partial y^4} \right) dx dy}{\iint_{\Delta A_j} \left(D_x \frac{\partial^4 w}{\partial x^4} + 2H \frac{\partial^4 w}{\partial y^2 \partial x^2} + D_y \frac{\partial^4 w}{\partial y^4} \right) dx dy} \quad (9)$$

Since both numerator and denominator, appeared in Eq. (9), are close to zero, this fraction is most susceptible to measurement and numerical errors. This is much more considerable for elements near support edges when element size and displacement are small. To remove this problem, the domain of interest in the problem is shifted by adding a unit value to the denominator and numerator of Eq. (9) (Stubbs *et al.* 2004).

$$1 = \frac{\iint_{\Delta A_j} \left(D_x^d \frac{\partial^4 w^d}{\partial x^4} + 2H^d \frac{\partial^4 w^d}{\partial y^2 \partial x^2} + D_y^d \frac{\partial^4 w^d}{\partial y^4} \right) dx dy + 1}{\iint_{\Delta A_j} \left(D_x \frac{\partial^4 w}{\partial x^4} + 2H \frac{\partial^4 w}{\partial y^2 \partial x^2} + D_y \frac{\partial^4 w}{\partial y^4} \right) dx dy + 1} \quad (10)$$

Eq. (10) can be written for all vibrating mode shapes of the plate. The summation of Eq. (10) for NMS available mode shapes can be expressed as follows

$$NMS = \sum_{i=1}^{NMS} \frac{\iint_{\Delta A_j} \left(D_x^d \frac{\partial^4 w_i^d}{\partial x^4} + 2H^d \frac{\partial^4 w_i^d}{\partial y^2 \partial x^2} + D_y^d \frac{\partial^4 w_i^d}{\partial y^4} \right) dx dy + 1}{\iint_{\Delta A_j} \left(D_x \frac{\partial^4 w_i}{\partial x^4} + 2H \frac{\partial^4 w_i}{\partial y^2 \partial x^2} + D_y \frac{\partial^4 w_i}{\partial y^4} \right) dx dy + 1} \quad (11)$$

Similarly, we can rewrite Eq. (5) for the mean of a shear force in x direction as follows

$$\bar{Q}_{xj} = \frac{1}{\Delta A_j} \iint_{\Delta A_j} Q_x dx dy = Q_{xy}(\hat{x}, \hat{y}) \quad (12)$$

Evaluating Eq. (5) at $x = \hat{x}$ and $y = \hat{y}$ substituting for $Q_x(x, y)$ using Eq. (3) yields

$$Q_{xy}(\hat{x}, \hat{y}) = \frac{-1}{\Delta A_j} \iint_{\Delta A_j} \frac{\partial}{\partial x} \left(D_x \frac{\partial^2 w}{\partial x^2} + H \frac{\partial^2 w}{\partial y^2} \right) dx dy \quad (13)$$

Similarly, for the damaged structure

$$Q_{xj}(\hat{x}, \hat{y}) = \frac{-1}{\Delta A_j} \iint_{\Delta A_j} \frac{\partial}{\partial x} \left(D_x^d \frac{\partial^2 w^d}{\partial x^2} + H^d \frac{\partial^2 w^d}{\partial y^2} \right) dx dy \quad (14)$$

With previous assumption, the shear force in x direction sum for the undamaged and damaged cases are equal too (this is true for statically determinate structures). So if we divide Eq. (14) to Eq. (13) then the result is expressed as

$$1 = \frac{\iint_{\Delta A_j} \frac{\partial}{\partial x} \left(D_x^d \frac{\partial^2 w^d}{\partial x^2} + H^d \frac{\partial^2 w^d}{\partial y^2} \right) dx dy}{\iint_{\Delta A_j} \frac{\partial}{\partial x} \left(D_x \frac{\partial^2 w}{\partial x^2} + H \frac{\partial^2 w}{\partial y^2} \right) dx dy} \quad (15)$$

Finally, after unity shift to the denominator and numerator of Eq. (15), to avoid the numerical error, and rewrite it for NMS available mode shapes. The summation of the results yields to

following expressions

$$NMS = \sum_{i=1}^{NMS} \frac{\iint_{\Delta A_j} \frac{\partial}{\partial x} \left(D_x^d \frac{\partial^2 w_i^d}{\partial x^2} + H^d \frac{\partial^2 w_i^d}{\partial y^2} \right) dx dy + 1}{\iint_{\Delta A_j} \frac{\partial}{\partial x} \left(D_x \frac{\partial^2 w_i}{\partial x^2} + H \frac{\partial^2 w_i}{\partial y^2} \right) dx dy + 1} \quad (16)$$

Similarly, for the y direction we have

$$NMS = \sum_{i=1}^{NMS} \frac{\iint_{\Delta A_j} \frac{\partial}{\partial y} \left(D_y^d \frac{\partial^2 w_i^d}{\partial y^2} + H^d \frac{\partial^2 w_i^d}{\partial x^2} \right) dx dy + 1}{\iint_{\Delta A_j} \frac{\partial}{\partial y} \left(D_y \frac{\partial^2 w_i}{\partial y^2} + H \frac{\partial^2 w_i}{\partial x^2} \right) dx dy + 1} \quad (17)$$

Having NMS , which is selected arbitrary, the i^{th} modal displacement of the undamaged plate w_i which is obtained through dynamic analysis and the i^{th} modal displacement of the damaged plate w_i^d which is obtained through field experiments, flexural rigidities in x and y directions for damaged state (D_x^d and D_y^d) and H^d will be obtained from Eqs. (11), (16) and (17). In this paper the required data of field experiments were provided via free vibration analysis of a simulated damaged plate with known damages. Then dynamic indices are expressed as follows

$$\beta_j = \frac{D_{xj}^d + D_{yj}^d}{D_x + D_y} \quad (18)$$

$$\beta_{xy} = \frac{D_{xj}^d}{D_x} \quad (19)$$

$$\beta_{yj} = \frac{D_{yj}^d}{D_y} \quad (20)$$

Using the above damage indices, possible locations of damage in the structure can be determined. Based on the magnitude of the damage index, for each element, a classification algorithm assigns each element into either a damaged or an undamaged category. Some classification schemes which have been already used in similar works can be named as (a) Bayes' rule (Gibson and Melsa 1975); (b) nearest distance (Nadler and Smith 1993); and (c) hypothesis testing (Ott 1993). In this study, hypothesis testing is utilized for the classification of an element as damaged or not damaged. In hypothesis testing, the alternate hypothesis ($H1$) and null hypothesis ($H0$) are defined as follows:

$H0$: Element j of the structure is not damaged

$H1$: Element j of the structure is damaged

To test the hypotheses, the damage indices shown in Eqs. (18), (19) and (20) are standardized using the Eq. (21).

$$Z_j = \frac{\beta_j^e - \mu_\beta}{\sigma_\beta} \quad (21)$$

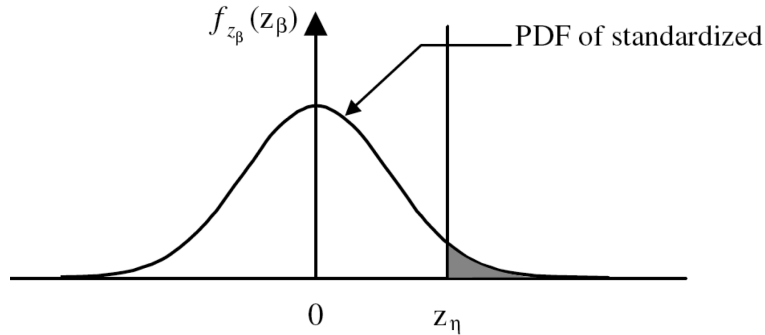


Fig. 2 Assumed probability density functions of standardized damage

where Z_j is the standardized damage index for the j^{th} element; μ_β and σ_β represent mean and standard deviation of the β_j^e , respectively. Assuming that the standardized damage index is normally distributed, a typical probability density function of the standardized damage indices depicted in Fig. 2 can be used for classification. Thus, the one-tailed test to decide on the existence of damage in the element j may be restated as follows:

- (i) Choose H0 if $Z_j < Z_\eta$, or
- (ii) Choose H1 if $Z_j \geq Z_\eta$

Is a threshold (Z_η is a threshold value) which assigns a confidence level for the presence of damage (Choi *et al.* 2005).

3. Numerical verification

In this section, feasibility and performance of the proposed NDD algorithm is examined by the aid of a numerical example. Fig. 1 shows the selected orthotropic plate example schematically. Plate dimensions are 70 cm length by 50 cm width and 0.3 cm thickness. The plate reinforced by 10 equidistance ribs in y direction. Therefore the flexural rigidities D_x , D_y , and H parameter can be calculated from the follow in expressions (Ventsel and Krauthammer 2001)

$$D_x = \frac{Eh^3}{12\left(1 - \frac{b}{t} + \frac{bh^3}{ts^3}\right)} \tag{22}$$

$$D_y = \frac{EI}{t} \tag{23}$$

$$H = \frac{Ch^3}{12} + \frac{C}{2t} \tag{24}$$

where I is the moment of inertia of a T-shaped section of width t (shown as shaded); C is the torsional rigidity of one rib about its centroidal axis. Other parameters have been shown in Fig. 3.

The plate is assumed to be four-edge clamped. Four-node plate elements are used to model the plate. The model has 80 elements (8×10), as shown in Fig. 4. The elements are numbered as

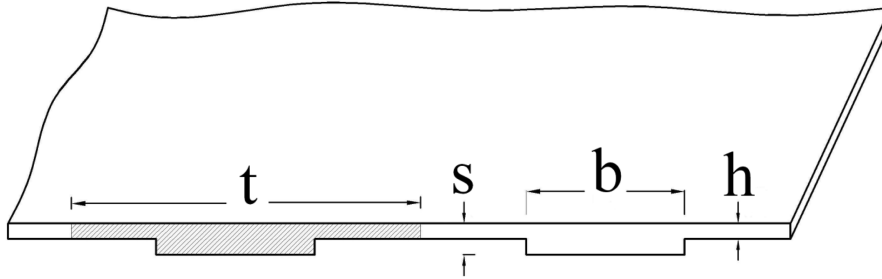


Fig. 3 Defined parameters for Eqs. (22)-(24)

1	2	3	4	5	6	7	8	9	10
11	12	13	14	15	16	17	18	19	20
21	22	23	24	25	26	27	28	29	30
31	32	33	34	35	36	37	38	39	40
41	42	43	44	45	46	47	48	49	50
51	52	53	54	55	56	57	58	59	60
61	62	63	64	65	66	67	68	69	70
71	72	73	74	75	76	77	78	79	80

Fig. 4 Element locations of the example plate structure

follows: Element 1 is in the top left corner of the plate, Element 80 is in the bottom right corner, and Element 10 is in the top right corner of the plate. The size of each element is $7\text{ cm} \times 6.25\text{ cm}$. All elements are assumed to be made of steel with $E = 215\text{ GPa}$, $\rho = 7850\text{ kg/m}^3$, $\nu = 0.3$. Free vibration analyses of both the damaged and undamaged plates are performed using a developed computer program (Gandomi 2008).

Since, to the naked eye the corresponding mode shapes for damaged structure are indistinguishable from undamaged one, only the mode shapes for the undamaged are shown in Fig. 5.

To verify the field applicability of the suggested methodology, the damage evaluation with incomplete and noisy data is conducted. Firstly, the effect of noise is simulated by adding a series of random noise generated from a uniform distribution on the interval $[-1, 1]$ to the original mode shapes of the plate. An $e\%$ random noise is added to the modal displacement vector as follows

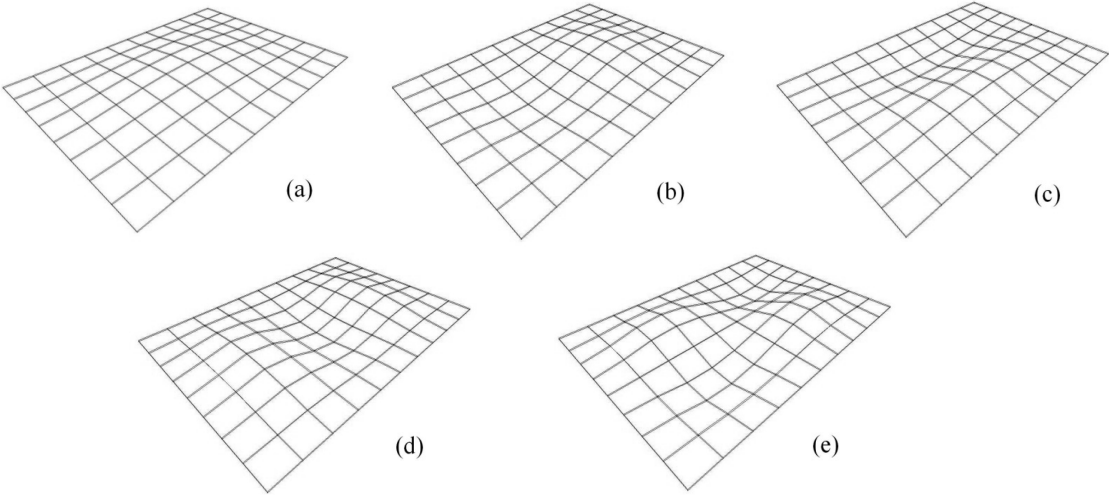


Fig. 5 Mode shapes of the orthotropic plate structure. (a) Mode 1, (b) Mode 2, (c) Mode 3 (d) Mode 4, (e) Mode 5 (There is no displacement and rotation in the plate boundaries)

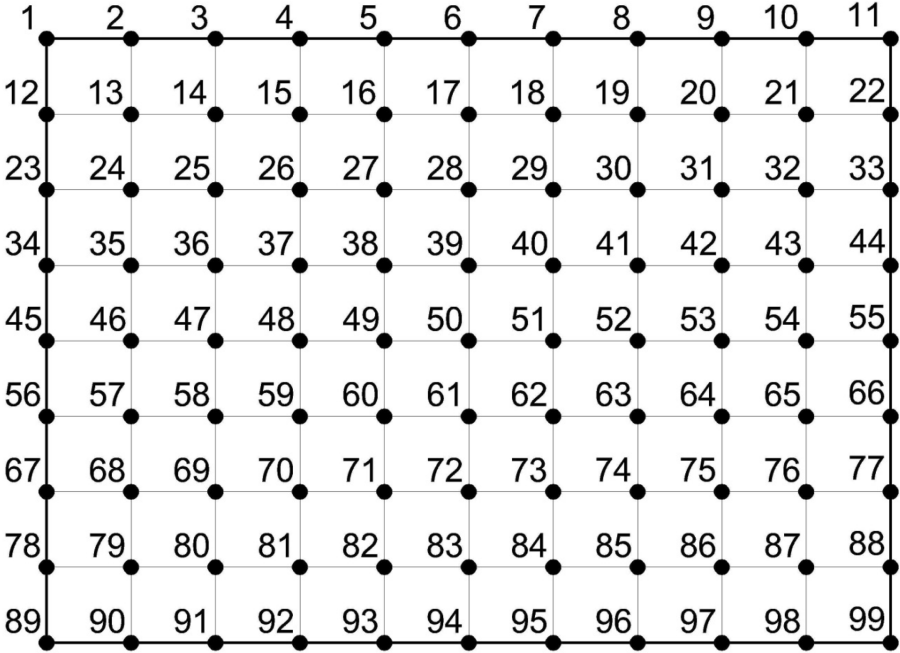


Fig. 6 Node locations of the example plate structure

$$\tilde{\phi}_j = \phi_j \left(1 + \frac{e}{100} \times \text{random noise} \right) \tag{25}$$

The effect of the incomplete modal data is simulated by performing damage detection using modal data from only 99 locations as depicted in Fig. 6.

The accuracy of the damage prediction can be quantified by such criteria as, the percentage of false positives (Type I error) and the percentage of false negatives (Type II error). A false positive means that damage is reported where no damage exists and a false negative means that damage is not reported where damage exists. The percentage of false positive error is calculated by dividing the number of false positive predictions by the number of undamaged elements, and the percentage of false negative error is calculated by dividing the number of false negative predictions by the number of damaged elements. The false positive and the false negative may reflect the quality of the measured data and the effectiveness of damage localization algorithm. Obviously, in an ideal situation, the false positive and the false negative error rates should be zero (Choi *et al.* 2006).

3.1 classification rules

After normalizing the pre-defined indices (Z_j , Z_{xy} and Z_{yj} are utilized for normalizing β_j , β_{xj} and β_{yj} , respectively), for isotropic and orthotropic damage states, the presence of damage in j^{th} element is determined according to the pre-assigned classification rules as the following:

- (a) the element is damaged if $Z_j \geq 1.24$;
- (b) the element is not damaged if $Z_j < 1.24$;

Note that the value of damage threshold, 1.24, corresponds to 90% confidence level for the presence of damage.

3.2 Different damage states

To evaluate the efficiency of the presented algorithm to locate the damages, different damage scenarios have been examined. In general depending on damage orientation in a plate structure, two different damage states which are isotropic and orthotropic damage can be considered.

In isotropic damages, the decrease of plate rigidity in two orthogonal directions is identical. In orthotropic damages two different magnitude of damage are induced. In this paper both two these cases have been studied. In addition in each state of isotropic and orthotropic damages, different number of elements with different damage magnitudes and different level of induced noise have been investigated. In total 48 damage cases for isotropic damage state and 40 damage cases are studied for orthotropic damage state.

3.2.1 Isotropic damage scenarios

In these damage scenarios, two different cases, which are plate with one and two damaged locations, are studied. Table 1 lists the damage scenarios and corresponding element numbers. These simulated locations can be found in Fig. 4. To examine the detectability of the algorithm for different damage levels, three damage magnitudes, i.e., 20, 30, and 50%, are simulated for each

Table 1 Simulated damage locations

Damage scenario	Elements damaged
1	45
2	39
3	35, 45
4	33, 55

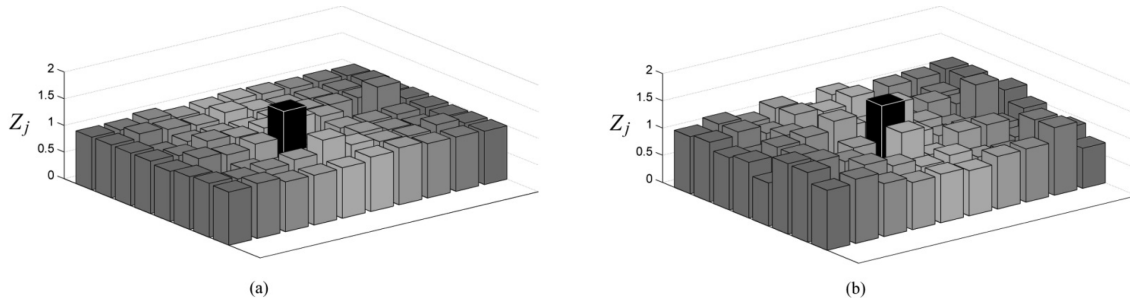


Fig. 7 Damage localization results for 1st Isotropic damage scenario (20% damage). (a) noise-free, (b) 2% noise

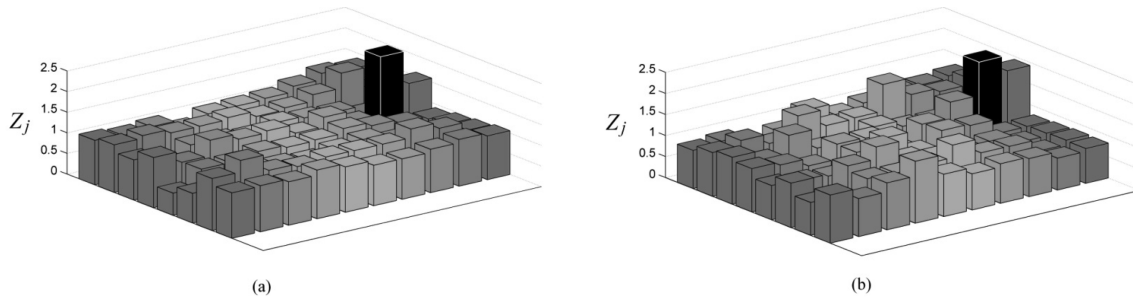


Fig. 8 Damage localization results for 2nd Isotropic damage scenario (50% damage). (a) noise-free, (b) 2% noise

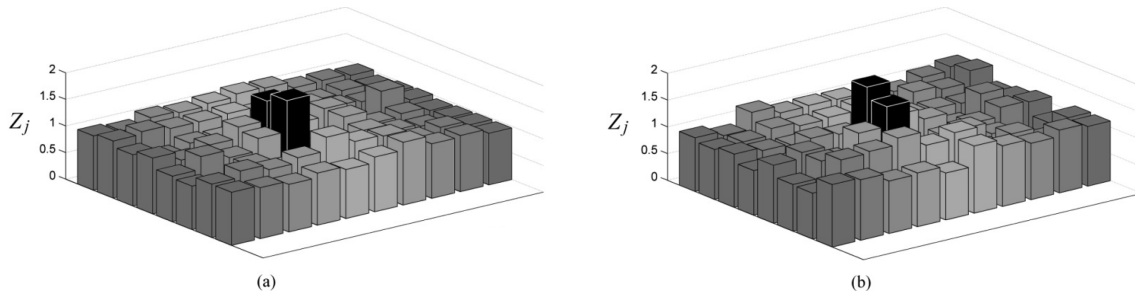


Fig. 9 Damage localization results for 3rd Isotropic damage scenario (30% damage). (a) noise-free, (b) 2% noise

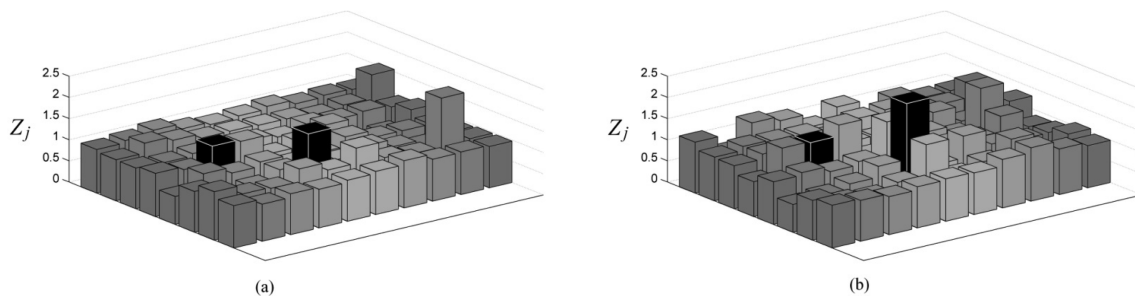


Fig. 10 Damage localization results for 4th Isotropic damage scenario (30% damage). (a) noise-free, (b) 2% noise

Table 2 Percentage of false positives and false negatives for isotropic damage state

Damage scenario	Severity	Percentage of False Positive				Percentage of False Negative			
		0% ^a	1%	2%	3%	0%	1%	2%	3%
1	20	2.5	6.25	12.5	18.75	0	0	0	0
	30	3.75	10	20	27.5	0	0	0	0
	50	12.5	13.75	22.5	30	0	0	0	0
2	20	0	6.25	15	23.75	0	0	0	0
	30	3.75	7.5	16.25	22.5	0	0	0	0
	50	7.5	13.75	20	27.5	0	0	0	0
3	20	2.5	10	15	18.75	0	0	0	0
	30	3.75	12.5	17.5	21.25	0	0	0	0
	50	10	13.75	17.5	22.5	0	0	0	0
4	20	5	7.5	13.75	16.25	0	0	0	0
	30	7.5	15	18.75	25	0	0	0	0
	50	8.75	15	20	27.5	0	0	0	0
Avg.		5.625	10.9375	17.39583	23.4375	0	0	0	0

^a noise/signal ratio.

damage scenario. To simulate the isotropic damage, the elastic modulus of the element corresponding to the location of the damage is reduced. Note that damage magnitude of 20% represents the 20% reduction in the elastic modulus of the element. Also four noise levels of 0%, 1%, 2% and 3% are imposed to simulated data. These are already used values by the other researchers (Choi *et al.* 1997, 2004, 2005, 2006).

In this Section, the Eq. (18) is utilized for detecting isotropic damages. After calculating the damage index for each element, the obtained damage index is standardized using Eq. (21). The damage localization results of each scenario are shown in Figs. 7 to 10 for free and 2% noises. The obtained standardized damage index for each element is presented in those figures. In all of the figures, the black columns indicate the inflicted locations of damage.

The percentage of false positive prediction and the percentage of false negative prediction are used to evaluate the ability performance of the methodology for isotropic damage state (see Table 2).

As it is observed, for all damage cases, the proposed methodology successfully identifies all simulated damage locations (notice to zero false negatives as shown in Table 2) for all noise and damage levels. As seen in the Table 2, the quantification of false positive is increasing as the noise level increases.

3.2.2 Orthotropic damage scenarios

In the orthotropic damage scenarios, damage location ranges from one to two locations. Table 3 lists the damage scenarios and corresponding element numbers. To examine the detectability of the algorithm for different damage levels, three damage magnitudes, i.e., 20, 30 and 50%, are simulated. To simulate the orthotropic damage, the flexural rigidities of plate in x and y directions have been changed independently. Table 4 shows damage severity for each damage scenario.

Table 3 Simulated damage locations and directions

Damage scenario	Elements damaged	Damage direction
1	45	X
2	45	Y
3	45	X and Y
4	35, 45	X
5	33, 55	Y

Table 4 Simulated damage directions and severity in each direction

Damage scenario	1		2		3		4		5	
Severity & Direction	30X	50X	30Y	50Y	20X 30Y	30X 50Y	30X	50X	30Y	50Y

Note that these simulated locations can be found in Fig. 4. Note that damage magnitude of 20X-30Y means the 20% and 30% reduction in the flexural rigidities in x and y directions of the element in respectively. Also four noise levels of 0%, 1%, 2% and 3% are imposed to simulated data.

In this Section, the Eqs. (18), (19) and (20) are utilized for detecting of orthotropic damages. After calculating the damage indices for each element, the obtained damage indices are standardized

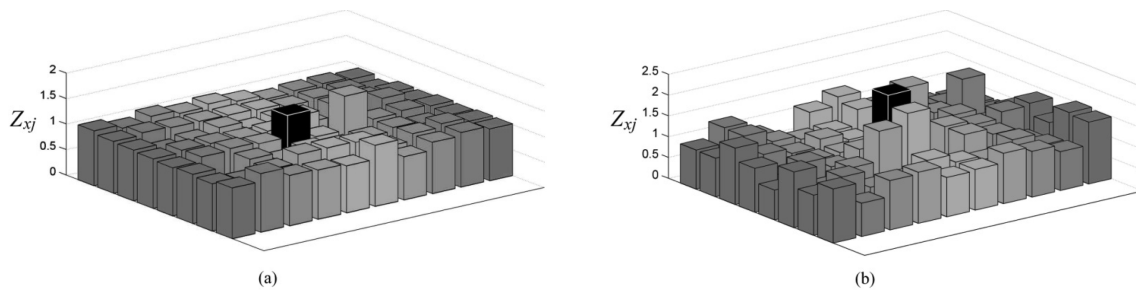


Fig. 11 Damage localization results for 1st Orthotropic damage scenario (30% damage in X direction). (a) noise-free, (b) 2% noise

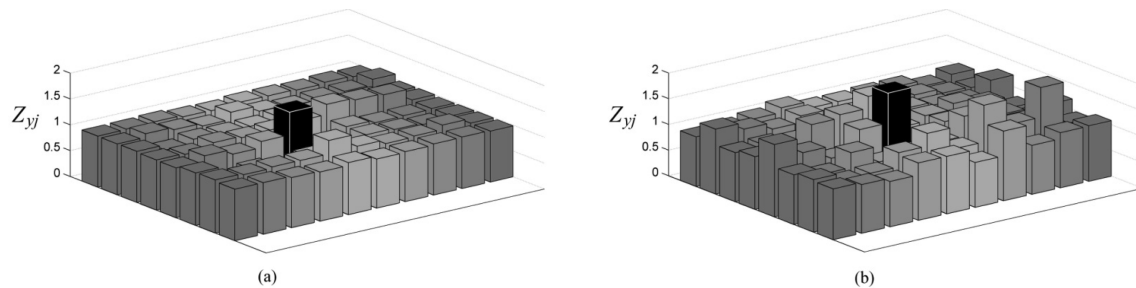


Fig. 12 Damage localization results for 2nd Orthotropic damage scenario (30% damage in Y direction). (a) noise-free, (b) 2% noise

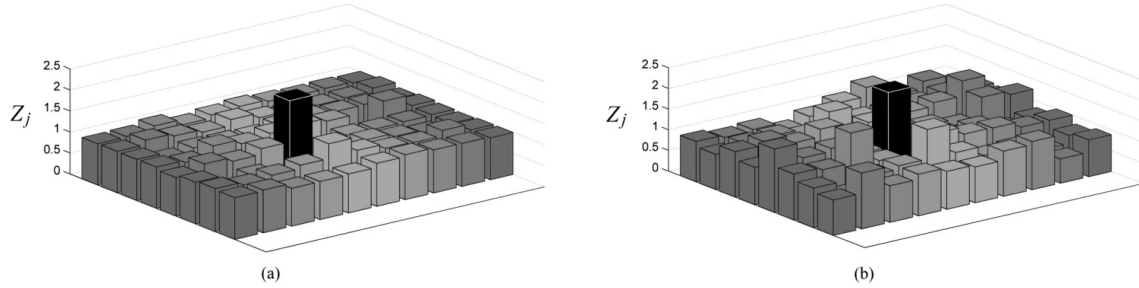


Fig. 13 Damage localization results for 3rd Orthotropic damage scenario (20% damage in X direction and 30% damage in Y direction). (a) noise-free, (b) 2% noise

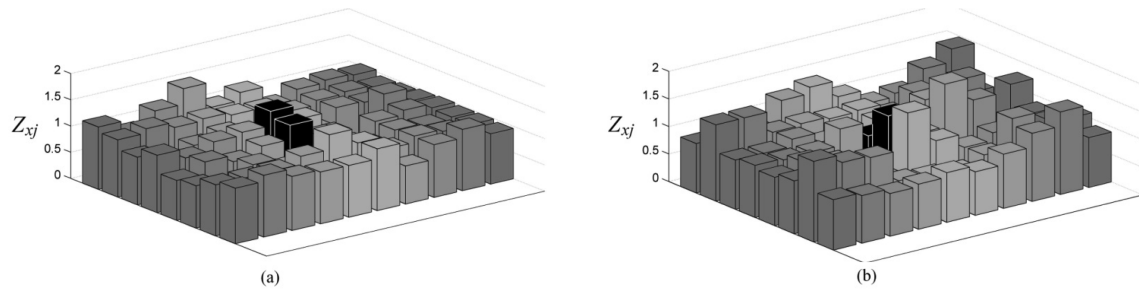


Fig. 14 Damage localization results for 4th Orthotropic damage scenario (30% damage in X direction). (a) noise-free, (b) 2% noise

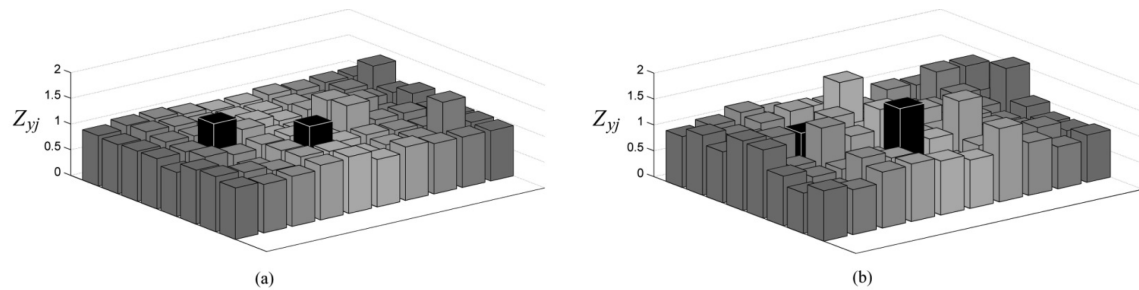


Fig. 15 Damage localization results for 5th Orthotropic damage scenario (30% damage in Y direction). (a) noise-free, (b) 2% noise

using Eq. (21). The damage localization results of each scenario are shown in Figs. 11 to 15 for free and 2% noises. The obtained standardized damage index for each element is presented in those figures. In all of the figures, the black columns indicate the inflicted locations of damage. The percentage of false positive prediction and the percentage of false negative prediction are used to evaluate the ability performance of the methodology for isotropic damage state (see Table 5).

As shown in Table 5, for the orthotropic damage state, the percentage of false negative prediction is increasing as the noise level increases. However, even with the highest noise level and the lowest damage magnitude, the proposed localization methodology identifies all damage locations except only two locations in damage cases of 4 and 5.

Table 5 Percentage of false positives, false negatives and utilized indices in each scenario for orthotropic damage state

Damage scenario	Severity	Percentage of False Positive				Percentage of False Negative				Index
		0% ^a	1%	2%	3%	0%	1%	2%	3%	
1	30X	1.25	3.75	15	17.5	0	0	0	0	β_{xj}
	50X	3.75	11.25	17.5	20	0	0	0	0	
2	30Y	2.5	8.75	15	25	0	0	0	0	β_{yj}
	50Y	5	11.25	15	25	0	0	0	0	
3	20X-30Y	3.75	7.5	15	21.25	0	0	0	0	β_j
	30X-50Y	5	10	12.5	18.75	0	0	0	0	
4	30X	7.5	12.5	21.25	25	0	0	50	50	β_{xj}
	50X	12.5	23.75	27.5	26.25	0	0	0	50	
5	30Y	5	7.5	15	18.75	0	0	50	100	β_{yj}
	50Y	7.5	8.75	12.5	15	0	0	0	0	
Avg.		5.375	10.5	16.625	21.25	0	0	10	20	

^anoise/signal ratio.

4. Conclusions

A damage identification methodology for plate structures, especially orthotropic plate structures was presented. This methodology utilized the third and fourth order derivatives of elastic surface in damaged and undamaged plate structure to identify the damages. The methodology was employed to detect and locate the damages in an exemplified orthotropic plate. Two kinds of damages i.e. orthotropic and isotropic damages were induced in this plate. Exact (free noise) and noisy numerically simulated measurements is used to evaluate the ability of the methodology of identify damages. From this study, the following conclusions are drawn:

1. Although the proposed methodology is able to find the damages in wide range of plate structures, it is especially able to detect and locate damages in orthotropic plates. It was shown that the methodology can detect both isotropic and orthotropic damages in plate structures.
2. The numerical study of a plate structure reveals that this methodology can identify single and multiple damage locations; and
3. The accuracy of the damage location using the methodology is decreased with noise-polluted data.

References

Araujo dos Santos, J.V., Mota Soares, C.M., Mota Soares, C.A. and Pina, H.L.G. (2000), "A damage identification: numerical model based on the sensitivity of orthogonality conditions and least squares techniques", *Comput. Struct.*, **78**, 283-291.

- Askeland, D.R. (1994), *The Science and Engineering of Materials*, PWS Publishing Company, Boston, USA.
- Cawley, P. and Adams, R.D. (1979), "The location of defects in structures from measurements of natural frequencies", *J. Strain Anal.*, **14**(2), 49-57.
- Chen, Y. and Swamidas, A.S.J. (1994), "Dynamic characteristics and modal parameters of a plate with a small growing surface crack", *Proceedings of the 12th International Modal Analysis Conference*, 1155-1161.
- Choi, S. and Stubbs, N. (1997), "Nondestructive damage detection algorithms for 2D plates", *SPIE Proceedings Smart Structures and Materials*, **3043**, 193-204.
- Choi, S., Park, S., Bolton, R., Stubbs, N. and Sikorsky, C. (2004), "Periodic monitoring of physical property changes in a concrete box-girder structure", *J. Sound Vib.*, **278**(1-2), 365-81.
- Choi, S., Park, S., Park, N. and Stubbs, N. (2006), "Improved fault quantification for a plate structure", *J. Sound Vib.*, **29**(3-5), 865-879.
- Choi, S., Park, S., Yoon, S. and Stubbs, N. (2005), "Nondestructive damage identification in plate structures using changes in modal compliance", *NDT & E Int.*, **38**(7), 529-540.
- Clough, R.W. and Penzien, J. (1995), *Dynamics of Structures*, 3rd Edition, McGraw-Hill Inc., New York, US.
- Cornwell, P., Doebling, S.W. and Farrar, C.R. (1999), "Application of the strain energy damage detection method to plate-like structures", *J. Sound Vib.*, **224**(2), 359-374.
- Doebling, S.W., Farrar, C.R., Prime, M.B. and Shevitz, D.W. (1996), *Damage Identification and Health Monitoring of Structural and Mechanical Systems from Changes in Their Vibrational Characteristics: A Literature Review*, Los Alamos National Laboratory, Los Alamos, [LA-13070-MS].
- Doherty, J.E. (1987), *Nondestructive Evaluation, Chapter 12 in Handbook on Experimental Mechanics*, (Ed. Kobayashi, A.S.), Society for Experimental Mechanics Inc., Englewood Cliffs, NJ.
- Gandomi, A.H. (2008), "A damage detection method in orthotropic plate structures", MSc Thesis, Iran, The Tafresh University, The Department of Civil Engineering, Iran.
- Gandomi, A.H., Sahab, M.G., Rahai, A. and Safari Gorji, M. (2008), "Development in mode shape-based structural fault identification technique", *World Appl. Sci. J.*, **5**(1), 29-38.
- Gibson, J.D. and Melsa, J.L. (1975), *Introduction to Nonparametric Detection with Applications*, Academic Press, New York, USA.
- Kaplan, W. (1991), *Advanced Calculus*, Addison-Wesley, Redwood City.
- Kim, B.H., Joo, H.J. and Park, T. (2006) "Nondestructive damage evaluation of a curved thin beam", *Struct. Eng. Mech.*, **24**(6), 665-682.
- Kim, J.T. and Stubbs, N. (1995a), "Damage detection in offshore jacket structures from limited modal information", *Int. J. Offshore Polar Eng.*, **5**(1), 58-66.
- Kim, J.T. and Stubbs, N. (1995b), "Model-uncertainty impact and damage-detection accuracy in plate girder", *J. Struc. Eng.*, **121**(10), 1409-1417.
- Lee, U., Kyoungkeun, C. and Shin, J. (2003), "Identification of orthotropic damages within a thin uniform plate", *Int. J. Solids Struct.*, **40**, 2195-2213.
- Nadler, M. and Smith, E.P. (1993), *Pattern Recognition Engineering*, Wiley, New York, USA.
- Ott, R.L. (1993), *An Introduction to Statistical Methods and Data Analysis*, Wadsworth, Belmont.
- Pandey, A.K., Biswas, M. and Samman M.M. (1991), "Damage detection from changes in curvature mode shapes", *J. Sound Vib.*, **145**, 321-332.
- Sohn, H., Farrar, C.R., Hemez, F.M., Shunk, D.D., Stinemates, D.W. and Nadler, B.R. (2003), *A Review of Structural Health Monitoring Literature: 1996-2001*, Los Alamos National Laboratory, Los Alamos, [LA-13976-MS].
- Stubbs, N. (1985), "A general theory of non-destructive damage detection in structures", *Proceedings of the Second International Symposium on Structural Control*, Martinus Nijhoff Publishers, Netherland.
- Stubbs, N., Kim, J.T. and Topole, K.G. (1992), "An efficient and robust algorithm for damage localization in offshore platforms", *Proceedings of the ASCE 10th Structures Congress '92*, 543-556.
- Stubbs, N., Kim, J.T. and Farrar, C.R. (1995), Field verification of a nondestructive damage localization and severity estimation algorithm, *Proceedings of the 13th International Modal Analysis Conference*, Nashville, TN, US.
- Stubbs, N., Park, S., Sikorsky, C. and Choi, S. (2000), "A global nondestructive damage assessment methodology for civil engineering structures", *Int. J. Syst. Sci.*, **31**(11), 1361-1373.

- Timoshenko, S.P. and Woinowsky-Krieger, S. (1959), *Theory of Plates and Shells*, 2nd Edition, McGraw-Hill Inc., New York, US.
- Ugural, A.C. (1999), *Stresses in Plates and Shells*, 2nd Edition, McGraw-Hill, New York, USA.
- Ventsel, E. and Krauthammer, T. (2001), *Thin Plates and Shells: Theory, Analysis, and Applications*, CRC Press, New York, USA.
- Yan, Y.J., Hao, H.N. and Yam, L.H. (2004), "Vibration-based construction and extraction of structural damage feature index", *Int. J. Solids Struct.*, **41**, 6661-6676.
- Yan, Y.J., Yam, L.H., Cheng, L. and Yu, L. (2006), "FEM modeling method of damage structures for structural damage detection", *Compos. Struct.*, **72**, 193-199.
- Yan, Y.J., Cheng, L., Wu, Z.Y. and Yam, L.H. (2007), "Development in vibration-based structural damage detection technique", *Mech Syst. Signal Pr.*, **21**(5), 2198-2211.
- Zhao, J. and DeWolf, J.T. (2007), "Modeling and damage detection for cracked I-shaped steel beams", *Struct. Eng. Mech.*, **25**(3), 131-146.
- Zou, Y., Tong, L. and Steven, G.P. (2000), "Vibration-based model-dependent damage (delamination) identification and health monitoring for composite structures", *J. Sound Vib.*, **230**(2), 357-378.